Available online at www.sciencedirect.com
SCIENCE DIRECT®
Journal of Molecular Catalysis A: Chemical 219 (2004) 301–308
JOURNAL OF MOLECULAR CATALYSIS A: CHEMICAL
www.elsevier.com/locate/molcata

Investigations on the novel niobium incorporated mesoporous catalytic materials

Deepak B. Akolekar*, Suresh K. Bhargava

Catalysis and Advanced Materials Research Group, Department of Applied Chemistry, RMIT University, P.O. Box 2476V, Melbourne, Vic. 3001, Australia

Received 4 March 2004; accepted 29 April 2004

Available online 3 July 2004

Abstract

High surface area novel niobium mesoporous catalysts were synthesised via sol–gel method. The Nb–Al–MCM-41 catalysts characterised by BET, FTIR, ICP-MS, XPS and XRD. The Nb–Al–MCM-41 samples exhibited very large surface area of 2285 m^2/g (pore volume 2.16 cm^3 g^{-1}) and 1550 m^2/g (pore volume 1.83 cm^3 g^{-1}) with average pore diameter of 37.9 Å (by BET) and 44.1 Å, respectively. The adsorption and disproportionation of NO and CO over Nb–Al–MCM-41 mesoporous catalysts indicated the formation of various NO/CO species or complexes with active metal sites. The structure-dynamics of the metal activated complex and reactive species formed during the CO/NO reaction has been studied. The nitrous oxide, nitrite, mononitrosyl, nitrate and dinitrosyl species formation were observed after the NO adsorption over the Nb–Al–MCM-41 catalysts. CO adsorption at room temperature lead to the formation of up to six bands attributed to physisorbed carbon dioxide and cationic Lewis acid carbonyl moieties as well as transition metal carbonyl complexes.

Keywords: FTIR; NO complexes; CO complexes; Nb–Al–MCM-41; Lewis acid sites; Active metal sites; XPS; BET

1. Introduction

The discharge of harmful substances from various sources causes air pollution, which are responsible for different environmental and health problems as such respiratory, cancer, birth defects, brain and nerve damage. The major pollutants (nitrogen oxide, carbon monoxide, carbon dioxide, sulphur dioxide and chlorofluorocarbons) above certain concentrations are extremely dangerous and can cause severe injury or death. Industrial and vehicular mobile sources are the major contributors for these pollutants. The hazardous gases like CO, NO and SO_2 released from industries and car exhausts are catalytically decomposed using noble metal catalysts [1–5]. In recent times, different transition metal systems have been employed with certain limitations for more effective and economical removal of the pollutants. The modified transition metal mesoporous and microporous materials often display unique selectivity in catalysis of these air pollutants [2–6].

The present environmental problems open up a challenge for the development of new catalytic materials. Mesoporous materials (M41S) are porous materials with regularly arranged, uniform mesopores ranging from 2 to 50 nm in diameter and large surface areas, which make them useful as adsorbents or catalysts. The MCM-41 material possesses a hexagonal array of uniform mesopores and usually synthesised with uniform channels varying from approximately 15 to >100 Å in size [7,8]. The transition metal mesoporous materials of type MCM-41 exhibits various excellent physico-chemical and catalytic properties [9,10]. In this study, we have developed new very high surface niobium containing mesoporous catalytic materials for CO and NO decomposition. So far the studies reported on high surface niobium mesoporous materials are limited. The main aims of this study were to prepare and characterise very high surface niobium containing mesoporous materials and determine the interactions towards the air pollutants such as nitric acid (NO) and carbon monoxide (CO). In situ infrared technique was employed for the elucidation of mechanisms

* Corresponding author.
E-mail addresses: deepak.akolekar@rmit.edu.au, E04781@ems.rmit.edu.au (D.B. Akolekar), suresh.bhargava@rmit.edu.au (S.K. Bhargava).

1381-1169/$ – see front matter © 2004 Elsevier B.V. All rights reserved.
doi:10.1016/j.molcata.2004.04.043

Table 1
Chemical and surface properties of the metal mesoporous catalysts

Catalyst	Si/Al	Si/Nb	Surface area (m^2/g)	Pore volume ($cm^3\,g^{-1}$)	Average pore diameter (by BJH desorption, D_{BJH}) (Å)	Average pore diameter (by BET) (Å)
Nb–MCM-41(a)	43.9	18.4	2285	2.16	40.3	37.9
Nb–MCM-41(b)	44.1	32.3	1550	1.83	36.8	44.1

of NO/CO reactions on niobium containing catalyst surfaces and type of active surface sites.

2. Experimental

2.1. Catalyst preparation

The niobium–Al–MCM-41 catalysts were prepared by hydrothermal synthesis of a mixture consisting of niobium salt solution, Ludox AS-40 (40 wt.% silica in water stabilized with ammonia), sodium aluminate solution, tetraethylammonium hydroxide (20 wt.%), cetyltrimethylamonium bromide (CTAB) and water. The synthetic mixture was prepared by mixing appropriate amount of Ludox, metal salt solution, sodium aluminate solution, tetraethylammonium hydroxide and CTAB for 3.0 h at room temperature. In the preparation of Nb–Al–MCM-41(I), the initial Si/Al and Si/metal ratios were 43 and 17 while in the Nb–Al–MCM-41(II), the initial Si/Al and Si/metal ratios were 43 and 34, respectively. After stirring was complete, the mixture was transferred to an Teflon coated autoclave and heated at 358 K for 190 h. During synthesis, pH was maintain between 11.0 and 12.1 was maintained using acid. The mesoporous material was thoroughly washed with de-ionised water, dried at 340 K for 29 h and calcined at 763 K for 18 h.

2.2. Catalyst characterisation

The chemical composition of the mesoporous catalysts was determined by ICP-MS using an Agilent Technologies 4500 series instrument. Surface area was obtained by the N_2-dynamic adsorption/desorption technique using a Micromeritics ASAP2000 instrument. Powder X-ray diffraction patterns were obtained with a Bruker D8 Advance XRD using a Ni-α filtered Cu Kα X-ray source. FTIR spectra were obtained using Perkin-Elmer System 2000 equipped with deuterated triglycine sulphate and mercury cadmium telluride detectors. FTIR studies were performed on self-supported wafer (ca. 20 mg) fixed to sample holder of a high temperature FTIR cell fitted with NaCl windows. All samples were first activated under vacuum ($<10^{-4}$ Torr) at 573 K for 16 h. A high purity mixture of nitrogen (95%) and nitric oxide (5%) and carbon monoxide (99.95%) supplied by Linde, Australia were used as the NO or CO source. The spectra of activated catalyst samples were used as a background from which the adsorbed probe molecule spectra were subtracted. All spectra were collected at room temper-

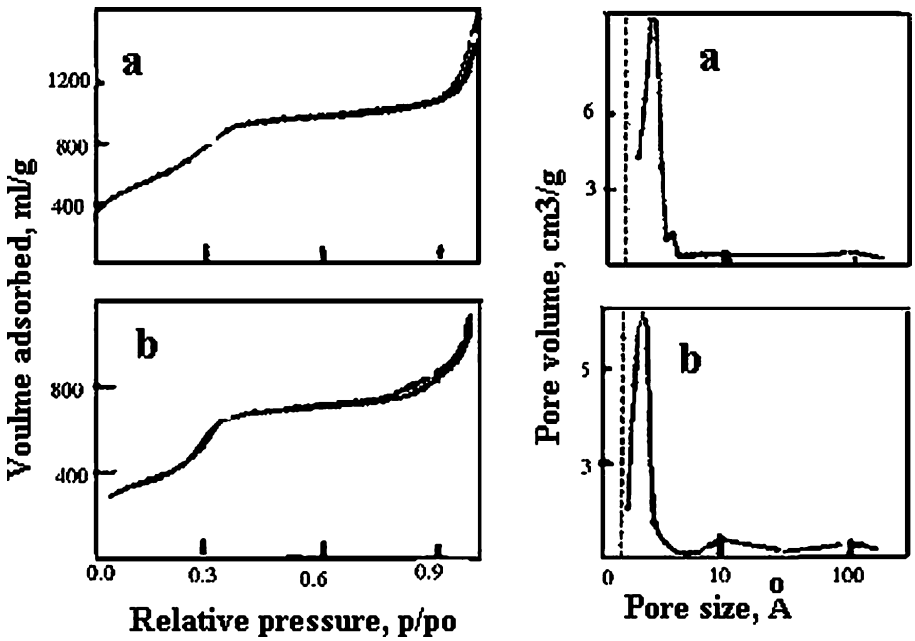

Fig. 1. N_2 isotherms and pore size distribution over the (a) Nb–Al–MCM-41(I) and (b) Nb–Al–MCM-41(II) catalysts.

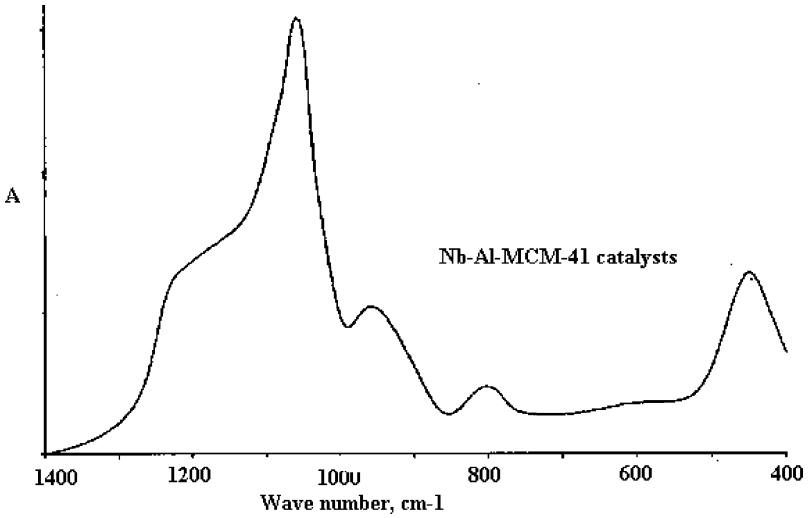

Fig. 2. FTIR spectra in the lattice vibration region of the Nb–Al–MCM-41 catalysts.

ature at different gas pressures and temperatures depending upon experimental conditions. FTIR spectra were obtained in the mid-infrared region, over the range 4000–1400 cm^{-1}, with 64 co-added scans at 2 cm^{-1} spectral resolution [3,4].

XPS surface analysis were conducted for determining the surface concentration and binding energy using a Fisons system (operated in the constant pass energy mode of 20 eV). An Mg Kα X-ray source ($h\nu = 1253.7$ eV) was operated at 20 mA and 15 mV. The base pressure of the instrument was 10^{-9} Torr. The intensity of the XPS band was determined using linear background subtraction and integration of peak areas. The binding energies were determined by computer fitting the measured spectra and were referenced to the C_{1s} at 285 eV.

3. Results and discussion

3.1. Properties of the niobium mesoporous catalysts

In this research study, we have prepared and characterised two different high surface niobium containing mesoporous catalysts and investigated their behaviour towards major air pollutants. The synthesised niobium containing mesoporous catalysts were highly crystalline and utilised for all the characterisation and FTIR studies. The characterisation of Nb–Al–MCM-41 materials by BET, ICP-MS and XRD confirmed the high phase purity. The in-house prepared niobium-containing mesoporous catalysts were of MCM-41 type as confirmed by the XRD (well defined XRD reflections (1 0 0), (1 1 0), (2 0 0)) and BET measurements. Powder X-ray diffraction shows typical reflections, characteristic of calcined MCM-41 materials at 2.1°, 2.5° and 4.2° (2Θ) [9–11]. The chemical properties and pore structure parameters of the niobium catalysts are presented in Table 1. The mesoporous catalysts were prepared with similar Si/Al ratio and different niobium loading for investigating their reactivity towards air pollutants and formation of the surface NO/CO species.

Fig. 1 shows the nitrogen sorption (BET) isotherm and pore size distribution for Nb–Al–MCM-41 materials. The BET data for these materials is presented Table 1. The Nb–Al–MCM-41(II) exhibits very surface area (2285 m^2/g) and large nitrogen sorption capacity (pore volume 1.83 $cm^3\,g^{-1}$) than the Nb–Al–MCM-41(I) (pore volume 2.16 $cm^3\,g^{-1}$, 1550 m^2/g surface area) which contains higher amount of niobium in the mesoporous material. The N_2 adsorption–desorption isotherms over the Nb–Al–MCM-41 catalysts (Fig. 1) are a type IV isotherm that is a typical of mesoporous material and the sharpness in isotherm steps is indicative of uniform pore size. For most of the catalysts, the pore size distribution curve shows a narrow pore size distribution with pore size of 44.1 Å for Nb–Al–MCM-41(I) and 39 Å for Nb–Al–MCM-41(II). The niobium incorporated mesoporous material exhibits very high surface area and pore volume as compared to the other transition (Co/Fe/Cu/Zn/Ni/Cr) metal incorporated materials [12]. Fig. 2 shows the mid FTIR spectrum of as-synthesised

Table 2
XPS analysis of the Nb–Al–MCM-41 mesoporous catalysts

Catalyst	Surface Si/Al ratio	Surface Si/Nb ratio	Binding energy, E_b (eV)[a]
Nb–Al–MCM-41(I)	54	27.4	$Nb_{3d\,5/2}$ 207.7, Al_{2p} 74.3, Si_{2p} 1031, O_{1s} 532.4
Nb–Al–MCM-41(II)	53	45.8	$Nb_{3d\,5/2}$ 208.1, Al_{2p} 74.2, Si_{2p} 103.3, O_{1s} 532.3

[a] Referenced to $C_{1s} = 285$ eV.

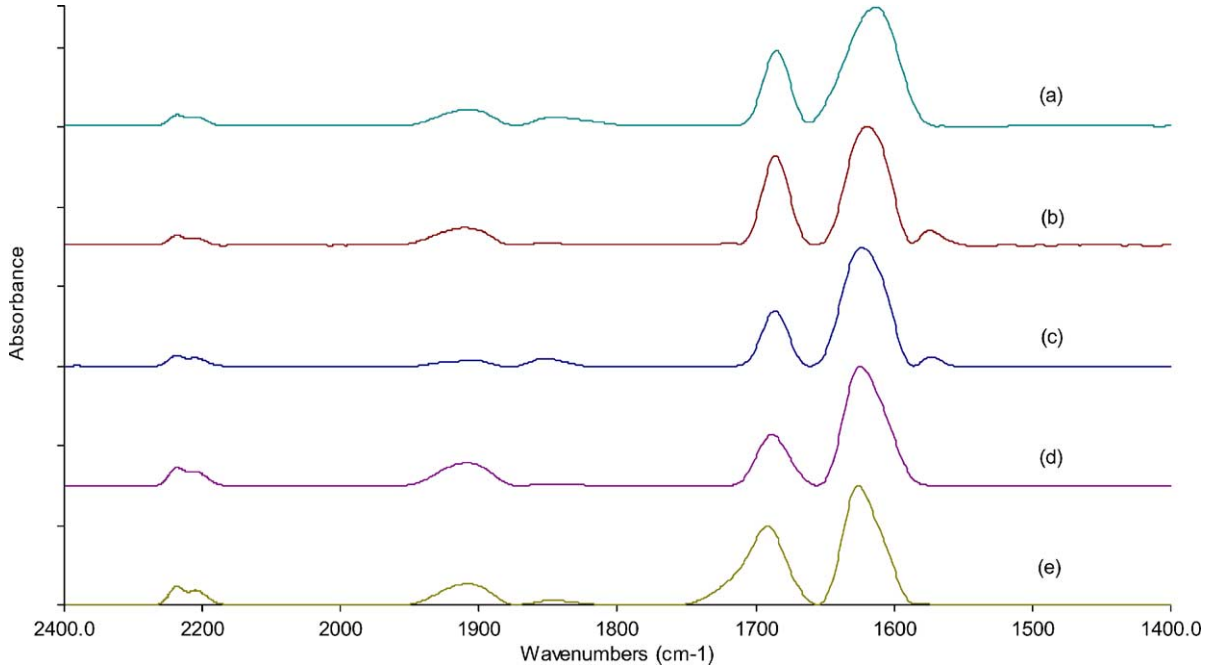

Fig. 3. FTIR spectra of NO adsorption on Nb–Al–MCM-41(I): (a) 22, (b) 61, (c) 103 Torr, (d), 423 K and (e) 523 K.

niobium mesoporous catalysts. The mid FTIR spectra are typical of mesoporous materials. The asymmetric stretching of framework Si–O–Si bonds was observed at 1090 cm^{-1}.

The surface concentration of the elements and the binding energy data for the Nb–Al–MCM-41 determined by XPS measurements are presented in Table 2. The results of bulk chemical (Table 1) and XPS surface (Table 2) analysis indicated that the Si:Al ratio on the surface is higher than that in bulk, which indicates that the concentration of aluminium is lower on the surface of these materials. Comparison of the bulk and surface Si:Nb ratio in the Nb–Al–MCM-41(I) and Nb–Al–MCM-41(II) indicated that the bulk concentration of the niobium atoms is higher than the surface of these materials and the niobium distribution is different in surface and bulk of the materials.

Table 2 presents the XPS binding energy data for the niobium mesoporous catalysts. The binding energy measured for Al_{2p} and Si_{2p} in the niobium mesoporous catalysts are

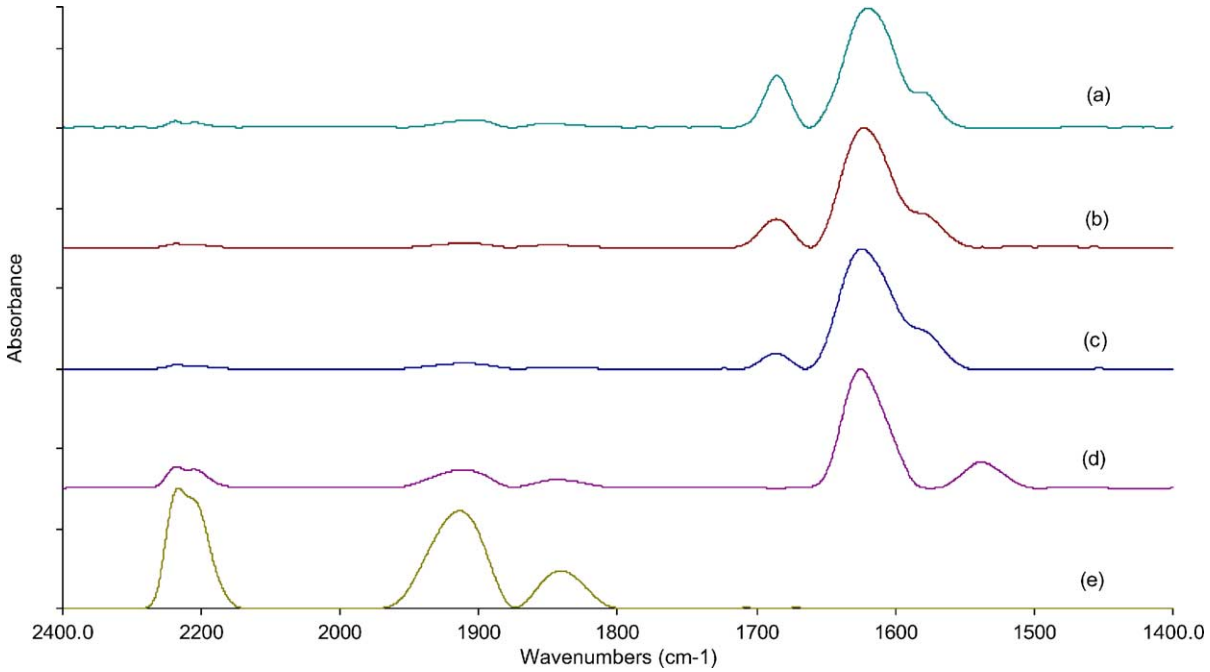

Fig. 4. FTIR spectra of NO adsorption on Nb–Al–MCM-41(II): (a) 22, (b) 61, (c) 103 Torr, (d) 423 K and (e) 523 K.

Table 3
Infrared band assignments for NO adsorption on the Nb–Al–MCM-41 mesoporous catalysts

Sample	NO pressure (Torr)	Temperature (K)	M-NO (cm^{-1})	M-$(NO)_2$ (cm^{-1})	M-NO_2 (cm^{-1})	M-N_2O (cm^{-1})	M-NO_3 (cm^{-1})
Nb–Al–MCM-41(I)	22	RT	1898	1855	1683 1620	2238	1578
	61	RT	1901	1851	1683 1622	2236	1578
	103	RT	1904	1848	1683 1624	2237	1579
	103	423	1907	1844	1624	2238	
	103	523	1910	1844		2237	
Nb–Al–MCM-41(II)	22	RT	1904	1853	1682 1614	2238	
	61	RT	1914		1684 1618	2236	1577
	103	RT	1897	1856	1682 1622	2237	1579
	103 (423 K)	423	1913		1688 1623	2238	1580
	103 (523 K)	523	1914	1843	1689 1623	2236	1579

similar to that of the tetrahedrally coordinated Al_{2p} and Si_{2p} in the zeolites and metal aluminophosphates [13,14]. The observed binding energies (~208 eV) of Nb and O_{1s} in the mesoporous catalysts are close to that of $Nb_{3d\,5/2}$ and O_{1s} in the niobium oxide in silicon dioxide-molybdenum matrix [13,15].

3.2. Interaction of NO with Nb–Al–MCM-41 catalysts

The interaction between NO and Nb–Al–MCM-41 catalysts is depicted in Figs. 3 and 4. The nature of sites, the oxidation state of the metal and the state and localisation of the cations on the catalyst surface are usually investigated using NO adsorption and a FTIR technique. After vacuum dehydration of the Nb–Al–MCM-41 in vacuo at 573 K for 16 h, exposure to NO resulted in up to six bands attributed to the formation of nitrous oxide (N_2O), chemisorbed nitrogen dioxide (NO_2), mononitrosyl (M-NO), dinitrosyl [M-$(NO)_2$], nitrite (M-NO_2), and nitrate (M-NO_3) complexes. The infrared bands assignment is consistent with the published literature [16–22]. The reactive O^- site reacts with another NO molecule to produce a M-NO_2

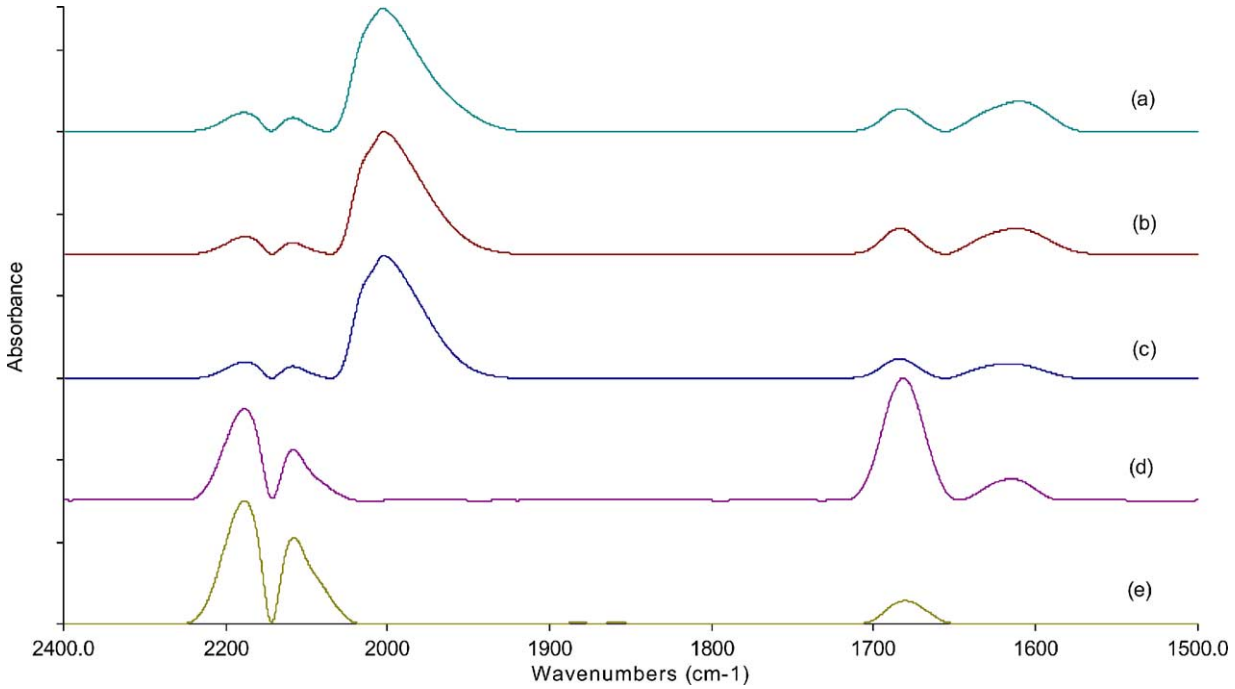

Fig. 5. FTIR spectra of CO adsorption on Nb–Al–MCM-41(I): (a) 22, (b) 61, (c) 103 Torr, (d) 423 K and (e) 523 K.

complex with a vibrational band at 1630 cm^{-1}. Nitrosyl species resulting from the reaction between nitric oxide and Nb–Al–MCM-41 are summarised in Table 3.

3.2.1. Effect of NO pressure on the adsorbed NO species

NO adsorption experiments at different pressures were carried out in order to study the influence of nitric oxide gas pressure on the niobium–nitric oxide complexes. FTIR results pertaining to the pressure changes of NO (that is, at different surface coverage) on the Nb–Al–MCM-41 are presented in Figs. 3a–c and 4a–c. Exposure to 22 Torr NO (Figs. 3a and 4a) produced six bands attributed to the formation of N_2O (2240 cm^{-1}), chemisorbed NO_2 (2170 cm^{-1}), M-NO (1900 cm^{-1}), M-$(NO)_2$ (1850 & 1730 cm^{-1}) and M-NO_2 (1630 cm^{-1}). Figs. 3a–c and 4a–c shows the changes in NO absorbance at different sites located on Nb–Al–MCM-41(I) and Nb–Al–MCM-41(II) catalyst at different pressures and constant temperature (296 K). At increasing NO pressure, the NO_x species concentrations at the respective bands (1900, 1850, 1730 and 1630 cm^{-1}) are significantly affected. Moreover the formation of N_2O (2238 cm^{-1}), and M-NO_2 (1630 cm^{-1}) species on the catalyst surface increased with the incremental dosage of NO. In addition, the conversion of the mononitrosyl to the dinitrosyl species is affected with the NO pressure as indicated by the changes in the intensity of asymmetric M-$(NO)_2$ band (1732 cm^{-1}). The Nb–Al–MCM-41(I) catalyst (Fig. 3), which contains higher amount of niobium, shows different concentration distribution of NO_x species than those on the lower niobium containing mesoporous (Nb–Al–MCM-41(II)) (Fig. 4) catalyst. In case of the low niobium (Nb–Al–MCM-41(II)) mesoporous catalyst, the concentration of the M-$(NO)_2$ decreases as seen by the decrease in the band intensity at 1850 & 1730 cm^{-1}.

3.2.2. Effect of temperature on the adsorbed NO species

The decomposition of adsorbed NO species at different temperatures and constant pressure over the dehydrated Nb–Al–MCM-41 catalysts is shown in Figs. 3c–e and 4c–e. Influence of temperature were investigated at a constant NO pressure (103 Torr) and at 423 and 523 K for 40 min. The NO_x species peak intensities as function of temperature showed interesting trends. By increasing the reaction temperature to 423 and 523 K (Figs. 3d and e, and 4d and e) the nitrate and nitrite moieties decomposed to mono and dinitrosyl species. In case of the Nb–Al–MCM-41(II), complete decomposition of the M-$(NO)_2$ (1730 cm^{-1}) and M-NO_2 (1630 cm^{-1}) occurred at 523 K. The presence of adsorbed N_2O and M-NO_2 bands indicates the oxidation of the niobium metal active sites. The changes in ratios of NO_x species indicated strong variation of the surface concentration and distribution of NO complexes with the temperature. Formation of a higher oxidation state species occurs when the dinitrosyl complex is oxidised by NO and forms an unstable complex with N_2O and O^- adsorbed species. Further reaction with NO leads to conversion of the unstable N_2O and O^- intermediates to a nitrite moieties. The reported disproportionation of NO reaction mechanism (by Giamello et al. [16] and Spoto et al. [17]) is in good agreement with the results. The dinitrosyl moiety (1850 cm^{-1} (asymmetric) and 1730 cm^{-1} (symmetric)) is formed by the adsorption NO molecule adsorbs onto M-NO at higher equilibrium pres-

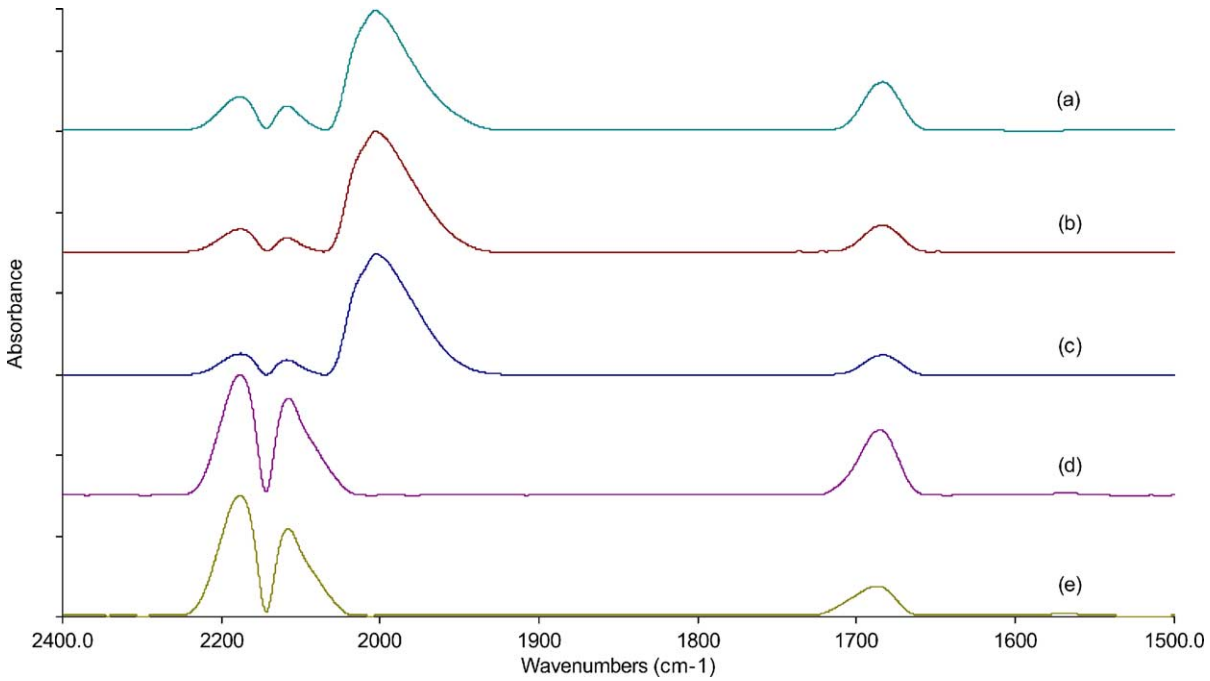

Fig. 6. FTIR spectra of CO adsorption on Nb–Al–MCM-41(II): (a) 22, (b) 61, (c) 103 Torr, (d) 423 K and (e) 532 K.

Table 4
Infrared band assignments for CO adsorption on the Nb–Al–MCM-41 mesoporous catalysts

Sample	CO pressure (Torr)	L-CO_a (cm^{-1})	L-CO_b (cm^{-1})	M-CO (cm^{-1})	M_3-CO (cm^{-1})	CO_2 (encapsulated) (cm^{-1})
Nb–Al–MCM-41(I)	22	2169	2118	2004	1682	1632
	61	2169	2117	2003	1683	1631
	103 (423 K)	2169	2117	2003	1681	1630
	103 (423 K)	2170	2117		1684	1632
	103 (523 K)	2171	2118		1683	
Nb–Al–MCM-41(II)	22	2168	2117	2004	1682	
	61	2169	2117	2004	1682	
	103	2170	2117	2003	1683	
	103 (423 K)	2171	2118			
	103 (523 K)	2170	2118			

L denotes cationic Lewis acid sites and M denotes active metal sites.

sure. The adsorption of NO molecule onto M-NO is usually followed by oxidation on the active metal catalyst [16,17]. The concentration of N_2O increased with the temperature on both the Nb–Al–MCM-41 catalysts.

3.3. Adsorption of CO on Nb–Al–MCM-41

Nb–Al–MCM-41 samples were used to investigate the interaction of CO using the in situ FTIR technique. The interaction between CO and Nb–Al–MCM-41 is presented in Figs. 5 and 6. After dehydration of Nb–Al–MCM-41 in vacuo at 573 K for 18 h, exposure to CO produced vibrational spectra with up to six infrared bands attributed to the formation of physisorbed carbon dioxide (CO_2), cationic Lewis acid carbonyl moieties (L-CO), linear and bridged transition metal carbonyl complexes (M-CO and M_x-CO). These infrared bands are consistent with the reported literature for microporous materials [4,18–25]. CO adsorption technique provides information about the oxidation and coordination state of charge balancing cations and widely employed for analysis of active sites on different materials. Table 4 presents the carbonyl transition metal complexes and intermediates resulting from surface reaction between carbon monoxide with the transition metal Al–MCM-41 mesoporous catalysts.

CO adsorption on activated Nb–Al–MCM-41 mesoporous catalysts at 298 K and increasing equilibrium pressures and temperatures is depicted in Figs. 5 and 6. At 22, 61 and 103 Torr, CO adsorption produced six infrared bands at 2169, 2118, 2060(sh), 2004, 1682 and 1632 cm^{-1} were observed on the Nb–Al–MCM-41(I) samples while the Nb–Al–MCM-41(II), which is lower in the niobium concentration, exhibited only four IR bands at 2168, 2117, 2004 and 1682 cm^{-1}. These bands are assigned to carbonyls associated with Lewis acid sites (L-CO) (2169, 2118 cm^{-1}), terminal transition metal carbonyls (M-CO) (2004 cm^{-1}), bridged transition metal carbonyls (M_x-CO) (1682 cm^{-1}) and encapsulated CO_2 (1632 cm^{-1}). The infrared band at 2169 cm^{-1} is assigned to CO adsorbed by the carbon on to cationic Lewis acid sites while the band at 2118 cm^{-1} is assigned to CO adsorbed on to Al–MCM-41 cationic Lewis acid sites by the oxygen atom. A weak shoulder band observed 2060 cm^{-1} is characteristic of terminal stretching CO vibrations present in metal-carbonyl species. In case of Nb–Al–MCM-41(I) and Nb–MCM-41(II) catalysts, above the reaction temperatures of 523 K, the terminal transition metal carbonyls (M-CO) (2004 cm^{-1}) species is decomposed. Only in the case of the Nb–Al–MCM-41(I), band related to encapsulated CO_2 (1632 cm^{-1}) is eliminated at the reaction temperature of 623 K. Niobium oxide has been used in various bi-functional catalysts due to its acidity. This supported catalyst possesses acidity and hydrogenation activity. In the Nb–silica catalysts, the part of Nb can be atomically dispersed on silica surface sue to formation of Nb–O–Si bond and the strong interaction between Nb atoms and silica leads to generation of Lewis acid sites detected by the higher positive charge on Nb atoms [15].

4. Conclusions

High purity niobium containing mesoporous materials (Nb–Al–MCM-41) were prepared with very high surface area and pore volume. NO adsorption on the Nb–Al–MCM-41 catalysts resulted in the formation of M-N_2O, M-NO, M-$(NO)_2$, M-NO_2 and M-NO_3 species. The NO pressure and reaction temperature significantly affects the concentration and distribution of NO species and conversion of nitrosyl species to nitrite and nitrate over the Nb–Al–MCM-41 catalyst. CO adsorption on the Nb–Al–MCM-41 mesoporous materials resulted in the formation of carbonyls predominantly associated with cationic Lewis acid sites. The main products formed from the interaction of CO with Nb–Al–MCM-41 catalysts are weakly adsorbed carbonyl species (CO) with vibrations at 2168 and 2118 cm^{-1}. The infrared band at 2169 cm^{-1} is assigned to CO adsorbed by the carbon on to MCM-41 tri-coordinated aluminium atoms (Lewis acid sites) while the band at 2118 cm^{-1} can be assigned to CO adsorbed by the oxygen on to MCM-41 Lewis acid sites. The concentration and distribution of CO species over the Nb–Al–MCM-41 cat-

alyst are strongly influenced by the CO pressure and the temperature.

Acknowledgements

The authors thank Dr. C. Kladis for the FTIR data collection.

References

[1] USEPA, APTI Course 482: Sources and Control of Volatile Organic Air Pollutants Student Workbook, EPA 450/2-81-011, 1981a.
[2] M. Iwamoto, Zeolites in environmental catalysis, Stud. Surf. Sci. Catal. 84 (1994) 1395.
[3] D.B. Akolekar, S.K. Bhargava, S.K. Stud, Surf. Sci. Catal. 105 (1998) 755.
[4] D.B. Akolekar, S.K. Bhargava, K. Foger, J. Chem. Soc., Faraday Trans. 94 (1) (1998) 155.
[5] M. Iwamoto, H. Yahiro, N. Mizuno, N. Mine, S. Kagawa, J. Phys. Chem. 95 (1991) 3727.
[6] Y. Li, N.J. Armor, Appl. Catal. 76 (1991) L1.
[7] C.T. Kresge, M.E. Leonwicz, W.J. Roth, J.C. Vartuli, J.S. Beck, Nature 359 (1992) 710.
[8] J.S. Beck, J.C. Vartuli, W.J. Roth, M.E. Leonwicz, C.T. Kresge, K.D. Schmitt, C.T.-W. Chu, D.H. Olson, E.W. Sheppard, S.B. McCullen, J.B. Higgins, J.L. Schlenker, J. Am. Chem. Soc. 114 (1992) 10834.
[9] M. Ziolek, I. Nowak, I. Sobczak, A. Lewandowska, P. Decyk, J. Kujawa, Stud. Surf. Sci. Catal. 129 (2000) 813.
[10] R. Kohn, D. Paneva, M. Dimitrov, T. Tsoncheva, I. Mitov, C. Minchev, M. Froba, Microporous Mesoporous Mater. 63 (1–3) (2003) 125–137.
[11] J.M. Kim, J.H. Kwak, S. Jun, R. Ryoo, J. Phys. Chem. 99 (1995) 16742.
[12] D.B. Akolekar, S.K. Bhargava, J. Colliod & Interface Sci. B, submitted for publication.
[13] D.B. Akolekar, J. Chem. Soc., Faraday Trans. 90 (7) (1994) 1041.
[14] M. Huang, A. Adnot, S. Kaliaguine, J. Catal. 137 (1992) 322.
[15] S. Damayanova, L. Dimitrov, L. Petrov, P. Grange, Appl. Surf. Sci. 214 (2003) 68.
[16] E. Giamello, D. Murphy, G. Magnacca, C. Morterra, Y. Shioya, T. Nomura, M. Anpo, J. Catal. 136 (1992) 510.
[17] G. Spoto, A. Zecchina, S. Bordiga, G. Richiardi, G. Mata, Appl. Catal. B Environ. 3 (1994) 151.
[18] K. Hadjiivanov, Catal. Rev.-Sci. Eng. 42 (2000) 71.
[19] C. Kladis, S.K. Bhargava, K. Foger, D.B. Akolekar, Catal. Today 63 (2000) 297.
[20] C. Kladis, S.K. Bhargava, K. Foger, D.B. Akolekar, J. Mol. Catal. A Chem. 171 (2001) 243.
[21] D.B. Akolekar, S.K. Bhargava, Appl. Catal. A General 207 (2001) 355.
[22] A. Zecchina, S. Bordiga, D. Scarano, G. Petrini, G. Leofanti, M. Padovan, C. Otero Arean, J. Chem. Soc., Faraday Trans. 88 (1992) 2959.
[23] V.S. Kamble, N.M. Gupta, V.B. Kartha, R.M. Iyer, J. Chem. Soc., Faraday Trans. 89 (1993) 1143.
[24] V.M. Rakic, R.V. Hercigonja, V.T. Dondur, Microporous Mesoporous Mater. 27 (1999) 27.
[25] K.I. Hadjiivanov, L. Dimitrov, Microporous Mesoporous Mater. 27 (1999) 49.